

Solution Enthalpy of Po and Te in solid Lead-Bismuth Eutectic

Kim Rijpstra^a, Andy Van Yperen-De Deyne^a, Jörg Neuhausen^b, Veronique Van Speybroeck^a, Stefaan Cottenier^{a,c,*}

^aCenter for Molecular Modeling, Ghent University, Technologiepark 903, BE-9052 Zwijnaarde, Belgium

^bLaboratory for Radio- and Environmental Chemistry, Paul Scherrer Institute, OFLB/101, CH-5232 Villigen PSI, Switzerland

^cDepartment of Materials Science and Engineering, Ghent University, Technologiepark 903, BE-9052 Zwijnaarde, Belgium

Abstract

It is examined to which extent first-principles calculations can be used to collect *a priori* information on the solution enthalpy and solubility of Po in solid lead-bismuth eutectic (LBE). Such information can be helpful to limit the number of complicated experiments that are required to measure these properties. It is found that in the thermodynamic limit and at 0 K, Po does not dissolve in solid LBE. Its solution enthalpy is negative, in particular in Pb-rich environments, but competing compound-forming reactions are more exothermic. A clear correlation is found between the calculated solution enthalpies for Te in LBE and for Po in LBE, suggesting that Te-experiments can be used to map the expected behaviour for Po. The role of spin-orbit coupling as the major relativistic effect on the solution enthalpies of these heavy atoms is inspected.

Keywords: first-principles calculations (DFT), liquid metal coolant, lead-bismuth eutectic (LBE), Polonium and Tellurium, solubility

1. Introduction

The molten phase of a Lead-Bismuth eutectic (LBE) is going to be used as coolant in planned experimental generation IV fission reactors [1]. Neutron capture by ²⁰⁹Bi will inevitably lead to the presence of a non-negligible amount of radiotoxic ²¹⁰Po in the coolant. For safety assessments, it is essential to know how this Po will interact with its environment in several operation and accident scenarios. Eventually, this has to be examined experimentally. However, exactly due to its radiotoxicity, Po-experiments are subject to major safety constraints and are therefore not straightforward to perform. In order to minimize the number of experiments, it would be convenient to know in advance as well as possible what to expect. This is a situation where predictive computational modeling can play a role. Indeed, it is well-established that many properties of molecules [2] and solids [3, 4, 5] can be predicted by solving the fundamental equations provided by quantum physics. In the case of solids, this is most often done in the framework of Density Functional Theory (DFT). The solution enthalpy of impurity elements in metals is one example of a property that can be determined by

DFT [6, 7, 8, 9, 10, 11, 12]. In this work, we will address the solution enthalpy of Po in solid LBE. We will do this in two ways: by directly predicting the solution enthalpy of a Po atom in solid LBE, and indirectly by dissolving the same amount of Te in exactly the same LBE-environment. The latter ‘virtual experiment’ will reveal a correlation between Po- and Te-behaviour, suggesting that it is possible to obtain information on Po in LBE by performing experiments on Te in LBE.

2. Computational details

All calculations in this work were done within the framework of Density Functional Theory [13, 14, 15, 16], using the Perdew-Burke-Ernzerhof exchange-correlation functional [17]. The numerical method used to solve the scalar-relativistic [18] Kohn-Sham equations for periodic solids is the Projector Augmented Wave (PAW) method [19, 20] as implemented in the VASP package [21, 3] (6-electron PAW potential for Te, d-electrons included for Pb, Bi and Po). Spin-orbit coupling as the major relativistic effect beyond the scalar-relativistic level was added for the calculations described in Sec. 5. The cut-off energy for the basis set size was taken to be 290 eV. The k-grids were Γ -centered Monkhorst-Pack grids, with a density of

*Stefaan.Cottenier@ugent.be

48 125 000 k-points/ \AA^{-3} . Both basis set size and k-point
 49 density were tested for numerical convergence. All unit
 50 cells were fully relaxed under the constraint of zero ap-
 51 plied pressure and all calculated energies therefore cor-
 52 respond to enthalpies. No entropic effects were taken
 53 into account, such that all quantities refer to the ground
 54 state (0 K). The calculations reported in this paper are
 55 equivalent to 10 cpu-years of single-core computing.

56 3. Elemental solids and LBE-model

57 Five solids will play a major role in this work: the el-
 58 elemental solids Te, Pb, Bi and Po, and a Pb-Bi mixture.
 59 In order to demonstrate the validity of the computational
 60 method for this kind of solids, we list in Tab. 1 some
 61 predicted basic structural properties for the elemental
 62 solids. The computational settings as described in Sec. 2
 63 were used. The bare calculated results were corrected
 64 for a systematic deviation as described in Ref. [5], and
 65 also the error estimates (1σ standard deviations) were
 66 taken from the latter work. The agreement between cal-
 67 culated and experimental values is reassuring for the
 68 validity of this computational method for this kind of
 69 solids. Furthermore, Tab. 1 demonstrates that spin-orbit
 70 coupling has a non-negligible effect on the properties of
 71 solids of heavy elements (see also Sec. 5).

72 Solid state DFT calculations require a unit cell as in-
 73 put, which is then periodically repeated to fill space. For
 74 an intrinsically disordered material as solid LBE, this
 75 straightforward approach is not possible. If it is the aim
 76 to describe the details of a disordered solid as faithfully
 77 as possible, one can resort to a set of elaborations or
 78 modifications of DFT that are meant for disordered al-
 79 loys [22]: special quasi-random structures (SQS) [23],
 80 cluster expansion [24] or the coherent potential method
 81 (CPA) [25]. Our aim, however, is to inspect whether and
 82 how the local stoichiometry of the nearest-neighbour
 83 shell affects the solution behaviour of Po. We there-
 84 fore take the simpler approach to describe a Pb-Bi alloy
 85 by a ‘disordered supercell’. A unit cell of the under-
 86 lying high-symmetry crystal structure is multiplied by a
 87 small integer factor in all three dimensions (in our case
 88 $2 \times 2 \times 2$, see Fig. 1-(a)), and all atom sites are randomly
 89 occupied by a predefined number of Pb and Bi atoms.
 90 Subsequently the shape and volume of the cell as well
 91 as the positions of the atoms are allowed to adjust them-
 92 selves in order to adopt the lowest-energy configuration
 93 under the condition of no applied pressure [12]. Apply-
 94 ing the same procedure to a $3 \times 3 \times 3$ cell would require
 95 100 times more computation time, and – as will be ar-
 96 gued in Sec. 4 – is bound to lead to the same conclusions

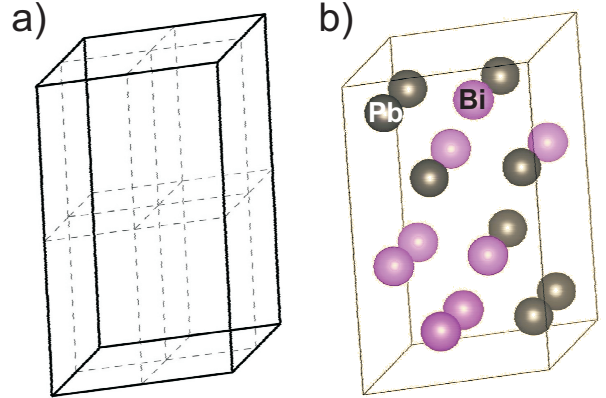


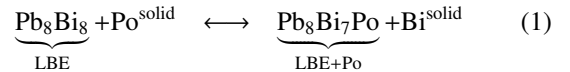
Figure 1: (a) A $2 \times 2 \times 2$ supercell of the hexagonal close packed primitive cell. (b) The randomly chosen Pb- and Bi-occupation that served as a model for a configurationally disordered Pb/Bi-alloy in this work.

97 as are obtained from the $2 \times 2 \times 2$ cell. For the same rea-
 98 son, only one random choice of the Pb/Bi-occupation is
 99 considered (see Sec. 4).

100 Which underlying crystal structure has to be taken for
 101 LBE? A glance at the Pb-Bi phase diagram in Fig. 2
 102 shows the relevant ones. Elemental Pb has the fcc struc-
 103 ture (cF4, Cu-type), and elemental Bi has a rhombohe-
 104 dral structure (hR6, As-type). Around the concentra-
 105 tion range of 70% Pb, the Pb-Bi mixture adopts the hcp
 106 structure (hP2, Mg-type). This hcp phase has a rather
 107 large homogeneity range. The solubility range of Pb
 108 in rhombohedral Bi is much smaller. In the broad con-
 109 centration range between 1 at.% and 57 at.% Pb, the
 110 material will consist of a mixture of almost pure Bi mi-
 111 crocrystals and hcp $\text{Pb}_{0.7}\text{Bi}_{0.3}$ microcrystals. Dissolving
 112 Po in LBE therefore means dissolving it in almost pure
 113 Bi and in hcp $\text{Pb}_{0.7}\text{Bi}_{0.3}$ (grain boundary effects are ne-
 114 glected). We want to examine how Po interacts with
 115 its immediate environment in Pb-Bi alloys. In order to
 116 sample as much as possible different nearest neighbour
 117 environments in a relatively small supercell, we take as
 118 our model system hcp- Pb_8Bi_8 . This means: 8 Pb-atoms
 119 and 8 Bi atoms are randomly distributed over the 16
 120 sites in a $2 \times 2 \times 2$ hcp supercell (Fig. 1-(b)).

121 4. Dissolving Po and Te in LBE

122 How much energy does it cost to put one Po atom in
 123 (the Pb-Bi microcrystals of) a LBE matrix? To answer
 124 this, we examine the reaction



	$V_0(\text{\AA}^3/\text{atom})$			$B_0(\text{GPa})$		
	Exp	no SO	SO	Exp	no SO	SO
Te	33.30	33.70 (1.1)	—	26.2	18.7 (15)	—
Pb	29.86	30.86 (1.1)	31.03 (1.1)	46.3	41.9 (15)	38.1 (15)
Bi	35.13	35.62 (1.1)	36.85 (1.1)	32.1	27.3 (15)	24.3 (15)
Po	36.93	36.16 (1.1)	38.04 (1.1)	27.4	48.2 (15)	37.3 (15)

Table 1: Equilibrium volume per atom (\AA^3) and equilibrium bulk modulus (GPa) for the bulk phases of Te, Pb, Bi and Po: experimental values (as listed in [5], extrapolated to 0 K and corrected for zero point motion), and calculated values (using the methods and settings described in Sec. 2) without (no SO) and with (SO) spin-orbit coupling. The calculated values have been corrected for the systematic deviations introduced by the PBE functional and an estimate of the expected uncertainty on the calculated value is given (see Ref. [5] for the procedure). Without spin-orbit coupling, all calculated volumes and bulk moduli agree with experiment within the error bar on the computed value, except for the bulk modulus of Po. When spin-orbit coupling is added, the latter disagreement is repaired.

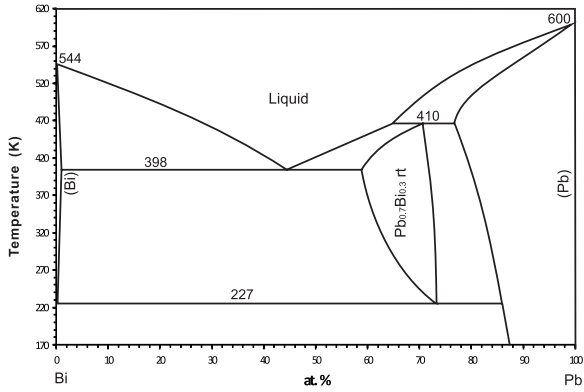


Figure 2: The Pb-Bi phase diagram as given in Ref. [26] (picture redrawn from AtomWork [27, 28]).

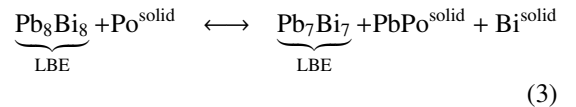
125 which describes solid Po (α -Po, simple cubic) in contact
126 with LBE (modeled by our 16-atom hexagonal cell), re-
127 acting to form solid bismuth and LBE with Po substituting
128 for a Bi atom. A similar reaction can be written for
129 Po substituting for Pb. The reaction enthalpy for Eq. 1
130 happens to be identical to the solution enthalpy of Po in
131 LBE:

$$\Delta H_{\text{sol}}^i = [H(\text{LBE} + \text{Po})_i + \mu_{\text{Pb}(\text{Bi})}] - [H(\text{LBE}) + \mu_{\text{Po}}] \quad (2)$$

132 It expresses the total enthalpy cost to remove one Po-
133 atom from a Po-reservoir with chemical potential μ_{Po} ,
134 to put it at a Pb (or Bi) site in LBE, and to bring the
135 replaced Pb-atom (or Bi-atom) to a Pb-reservoir (or Bi-
136 reservoir) with chemical potential μ_{Pb} (or μ_{Bi}). For the
137 reservoirs (or chemical potentials μ), one usually takes
138 the enthalpy per atom in the elemental solids, i.e. as de-
139 termined by the calculations described in Sec. 3.

140 One after the other, all 16 Pb or Bi atoms in our model
141 LBE are replaced by a Po atom, after which the super-

142 cell is allowed in all cases to relax completely. This re-
143 sults in 16 different values for the enthalpy $H(\text{LBE} + \text{Po})_i$
144 ($1 \leq i \leq 16$). These 16 solution enthalpies are plotted
145 in Fig. 3-(a) as a function of the number of Pb atoms
146 in the first coordination shell of Po. The same picture
147 shows the solution enthalpy for Po in rhombohedral Bi
148 and fcc-Pb as well. The solution enthalpy for Po in Pb is
149 positive, indicating that at 0 K Po will not dissolve spon-
150 taneously in Pb. For Po in Bi, the (scalar-relativistic)
151 solution enthalpy is slightly positive as well. For Po in
152 LBE, there is a rough trend with respect to the number
153 of Pb neighbours: Po has a positive solution enthalpy
154 when it goes to sites with few Pb neighbours, and a neg-
155 ative solution enthalpy when it goes to sites with many
156 Pb neighbours. This negative solution enthalpy means
157 that the reaction in Eq. 1 will proceed exothermally to
158 the right if Po ends up in an environment with a lot of
159 Pb-atoms. It does not mean, however, that Po will effec-
160 tively dissolve into the solid Pb/bi-microcrystals in LBE
161 in Nature. For this to happen, there should be no alter-
162 native reaction that is even more exothermal. As solid
163 PbPo is experimentally known to exist in the rocksalt
164 structure [29], a straightforward alternative that should
165 be examined is



166 The reaction enthalpy for this reaction is calculated to
167 be -0.60 eV/Po , which is clearly lower than the low-
168 est value of -0.27 eV/Po in Fig. 3-(a) (or Eq. 1). As
169 a consequence, Po will not dissolve spontaneously into
170 solid LBE ¹. Either it will react with LBE to form

¹As -0.60 eV is considerably lower than -0.27 eV , this conclusion will not be affected by taking a different random occupation for the 16-atom LBE cell, or by taking a larger supercell to model LBE.

171 rocksalt PbPo and rhombohedral Bi, or it will follow 223
 172 other reaction paths that have even more negative reac- 224
 173 tion enthalpies (involving, for instance, ternary Pb-Bi- 225
 174 Po phases). This conclusion is consistent with exper- 226
 175 imental observations that Po inside solid Pb [30] and 227
 176 solid LBE [31, 32] migrates to the surface and/or to 228
 177 grain boundaries [33]. 229

178 Exactly the same procedure was followed to deter- 230
 179 mine the solution enthalpy of Te in LBE. This results 231
 180 in Fig. 3-(b) for a reaction similar to Eq. 1. The solu- 232
 181 tion enthalpy for Te in solid Pb is positive, consis- 233
 182 tent with the low solubility range of Te in Pb [34]. At 234
 183 the Bi-side, the solution enthalpy is slightly negative. 235
 184 Yet, in low-temperature experiments Te will not dis- 236
 185 solve in rhombohedral Bi, as it is more favourable to 237
 186 form Bi_4Te_3 [35]. This too is consistent with the low 238
 187 solubility range of Te in Bi (0.2 at.% at most [36]). The
 188 solution enthalpy of Te in the Pb/Bi-microcrystals of
 189 LBE is considerably negative (down to -0.40 eV/Te),
 190 and Te prefers Pb-rich environments in LBE, just as
 191 Po does. Te is not expected to dissolve effectively into
 192 LBE, however, as also here at least one competing reac-
 193 tion can be found with a lower reaction enthalpy: the
 194 analogue of Eq. 3 with PbTe has a reaction enthalpy of
 195 -0.96 eV/Te. PbTe is indeed the phase that is found ex-
 196 perimentally [37, 38, 39].

197 At this point, one can exploit a particular feature of
 198 first principles calculations: the ability to do very con-
 199 trolled ‘experiments’ in a way that is not achievable
 200 in a lab. Using the 2×18 data points in both Fig. 3-
 201 (a) and Fig. 3-(b), we can compare the enthalpy cost
 202 of putting either Po or Te in *the same* atomistic envi-
 203 ronment (i.e. identical coordination symmetry, differ-
 204 ent bond lengths). If these two data sets are plotted
 205 with respect to each other, an excellent linear correlation
 206 emerges (Fig. 4). In order to test whether or not this cor-
 207 relation depends on the particular $2 \times 2 \times 2$ LBE-model we
 208 have chosen, data points for reaction enthalpies of other
 209 crystals in contact with solid Te or solid Po were calcu-
 210 lated: Te/Po as impurity in fcc Pb (concentrations of
 211 3.1%, 6.25% and 25%), Te/Po as impurity in rhombo-
 212 hedral Bi (4.2%), substitution of all Pb in hypothetical
 213 Bi_4Pb_3 by Te/Po, and substitution of either all Pb or all
 214 Bi in hypothetical rocksalt PbBi by Te/Po. As Fig. 4
 215 shows, these data points obtained in very different crys-
 216 tals perfectly follow the linear correlation. This strongly
 217 suggests that this linear correlation is a genuine prop-
 218 erty, and not an artefact due to the limited $2 \times 2 \times 2$ LBE
 219 supercell or the single random configuration. The linear
 220 correlation in Fig. 4 implies that Te is more strongly
 221 bound to the LBE matrix than Po is: environments that
 222 bind Te by less than 0.09 eV per solute atom, do not

bind Po any longer (less than 0.14 eV per solute atom if
 spin-orbit coupling is considered). The latter is consis-
 tent with experimental observations in solid PbTe and
 solid PbPo (rock salt structure): whereas PbTe melts at
 1195 K [40], PbPo decomposes already between 820
 and 900 K [41, 42] or sublimates around 1000 K [29]. An-
 other corroborating observation is the evaporation rate
 of Po from LBE, which is larger than the one of Te from
 LBE [43].

Knowing this correlation, it would be possible to pre-
 dict the solution enthalpy of Po in any LBE-like envi-
 ronment without making a DFT calculation, provided
 one has calculated the solution enthalpy of Te in that
 same environment. By extension, this applies to exper-
 iment as well: performing experiments on Te in LBE
 provides information that in principle could be trans-
 lated to Po in LBE.

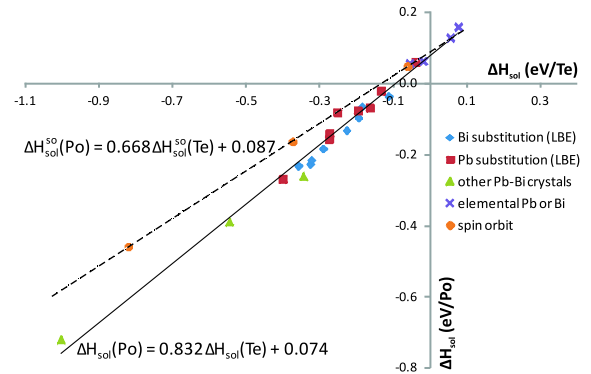


Figure 4: Correlation between the solution enthalpies of Po and Te in LBE (1/16), elemental Pb (various concentrations), and in elemental Bi (1/24). Additionally, the same correlation for full substitution of either Pb or Bi by Po or Te is given for PbBi (NaCl-structure) and for Bi_4Pb_3 . Every data point corresponds to a different local environment for Po/Te. In the two calculations that lead to every data point, all atomic positions were independently optimized (=the distance between Te and its neighbours is allowed to be different from the distance between Po and its neighbours). The dashed line is a similar fit through three well-separated data points, now taking spin-orbit coupling into account (from left to right: Bi-substitution in PbBi [NaCl], Pb-substitution in PbBi [NaCl], 25% of Po/Te in fcc-Pb).

5. Influence of spin-orbit coupling

The common way to perform DFT calculations is to do it at the scalar-relativistic level [18]. This includes, for instance, the speed dependence of the mass of the electron. For heavy atoms, relativistic effects beyond the scalar-relativistic level cannot be entirely neglected. The dominant effect is spin-orbit coupling, which can be added in a perturbative way to scalar-relativistic calculations. Tab. 1 demonstrates the impact of spin-orbit

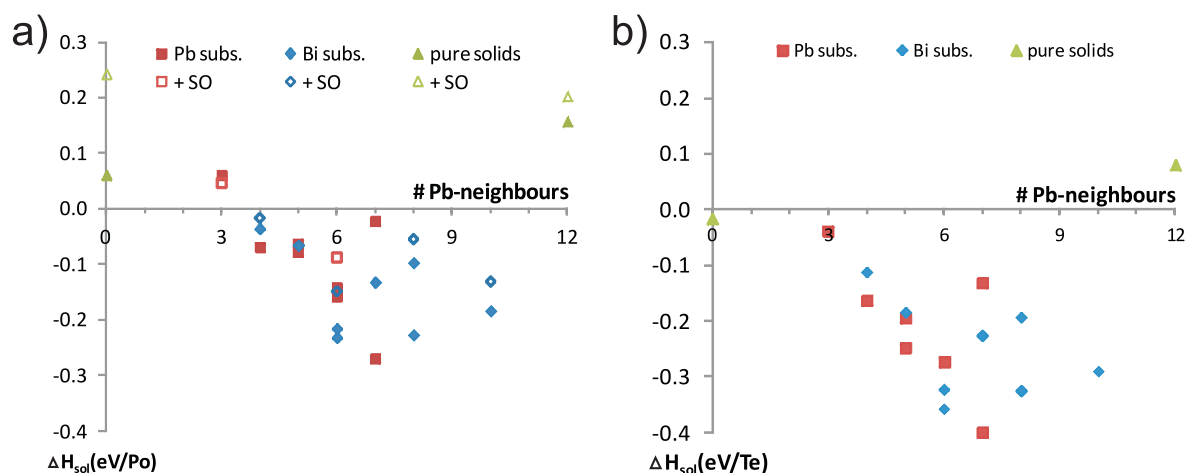


Figure 3: (a) Solution enthalpy for Po at all 16 positions in our LBE model, as well as in pure Bi and pure Pb. These solution enthalpies are plotted with respect to the number of Pb-neighbours in the first coordination shell of Po. Open symbols are data points for which spin-orbit coupling has been taken into account. (b) Idem, but for Te instead of Po.

249 coupling on the equilibrium volume and bulk modulus of the pure phases of Pb, Bi and Po: without spin-orbit coupling, all calculated volumes and bulk moduli agree with experiment within the error bar on the computed value, except for the bulk modulus of Po. When spin-orbit coupling is added, the latter disagreement is repaired. Therefore, we did apply spin-orbit coupling to some of the Po-substitutions in LBE. The result is that the scalar-relativistic solution enthalpies are shifted in the direction of more positive values by a varying amount, that has the order of magnitude of 0.1 eV per solute atom (open symbols in Fig. 3-(a)). This shows that the Po solution enthalpy is less negative than the scalar-relativistic calculations suggested. However, the qualitative conclusions are not affected (no dissolution in the pure materials, Pb-rich environments preferred in LBE). For three well-separated points in Fig. 4, all calculations were repeated with spin-orbit coupling (including the geometry optimization). This allows to determine the linear correlation with spin-orbit coupling taken into account (dashed line in Fig. 4). It is this line which should be used to convert experimental solution enthalpies for Te into predicted solution enthalpies for Po.

273 6. Conclusions

274 Starting from a simple model system for solid LBE and using only information obtained from first-principles calculations, we predict that at low temperatures Po will not dissolve in the matrix of solid LBE (grain boundary solution was not studied). Although

279 its solution enthalpy is negative (and most so in Pb-rich environments), competing compound-forming reactions are more exothermic. Similar calculations for Te in LBE show that Te is bound stronger by the LBE matrix than Po is. Solution enthalpies for Te in LBE correlate strongly with solution enthalpies for Po in LBE. This suggests that Te experiments can be used to map the expected behaviour for Po, a procedure that can reduce the number of required Po experiments.

288 Acknowledgement

289 This work is supported by the European Commission through the FP7 project SEARCH (Safe ExploitAtion Related CHemistry for HLM reactors, project nr. 295736) and by the Research Board of Ghent University. The authors acknowledge helpful discussions with Alexander Aerts (SCK-CEN, Mol), Emilio Andrea Maugeri and Matthias Rizzi (both PSI, Villigen). Three anonymous referees have contributed valuable suggestions. Stefaan Cottenier acknowledges financial support from OCAS NV by an OCAS-endowed chair at Ghent University. Calculations were carried out using the Stevin Supercomputer Infrastructure at Ghent University, funded by Ghent University, the Hercules Foundation, and the Flemish Government (EWI Department).

- 304 [1] H. A. Abderrahim, P. Baeten, D. De Bruyn, R. Fernandez, Energy Conversion And Management 63 (2012) 4–10.
- 305 [2] Pekka Pyykkö, John F. Stanton (Eds.), Chemical Reviews 112 (2012) 1–672.
- 306 [3] J. Hafner, Journal of Computational Chemistry 29 (2008) 2044.

- 309 [4] K. Schwarz, P. Blaha, S. Trickey, *Molecular Physics* 108 (2010) 3147. 374
- 310 317
- 311 [5] K. Lejaeghere, V. V. Speybroeck, G. V. Oost, S. Cottenier, *Critical Reviews in Solid State Physics and Materials Science* (2013). 376
- 312 377
- 313 [6] D. Jiang, E. A. Carter, *Physical Review B* 67 (2003) 214103. 378
- 314 [7] C. Wolverton, V. Ozolins, M. Asta, *Physical Review B* 69 (2004) 144109. 379
- 315 380
- 316 [8] C. Wolverton, V. Ozolins, *Physical Review B* 73 (2006) 144104. 381
- 317 [9] F. Soisson, C. Fu, *Physical Review B* 76 (2007) 214102. 382
- 318 [10] P. Erhart, B. Sadigh, A. Caro, *Applied Physics Letters* 92 (2008) 141904. 383
- 319 384
- 320 [11] A. Harutyunyan, N. Awasthi, A. Jiang, W. Setyawan, E. Mora, T. Tokune, K. Bolton, S. Curtarolo, *Physical Review Letters* 100 (2008) 195502. 385
- 321 386
- 322 [12] K. Lejaeghere, S. Cottenier, S. Claessens, M. Waroquier, V. V. Speybroeck, *Physical Review B* 83 (2011) 184201.
- 323 324
- 325 [13] P. Hohenberg, W. Kohn, *Physical Review* 136 (1964) B864.
- 326 [14] W. Kohn, L. J. Sham, *Physical Review* 140 (1965) A1133.
- 327 [15] R. Martin, *Electronic Structure. Basic Theory and Practical Methods*, Cambridge University Press, 2004.
- 328 329
- 330 [16] S. Cottenier, *Density Functional Theory and the Family of (L)APW-methods: a step-by-step introduction*, (Instituut voor Kern- en Stralingsfysica, KULeuven, Belgium), 2002. ISBN 90-807215-1-4 (freely available from http://www.wien2k.at/reg_user/textbooks).
- 331 332 333
- 334 [17] J. P. Perdew, K. Burke, M. Ernzerhof, *Physical Review Letters* 77 (1996) 3865.
- 335 336
- 337 [18] D. Koelling, B. Harmon, *J. Phys. C: Solid State Phys.* 10 (1977) 3107.
- 338 [19] P. E. Blöchel, *Physical Review B* 50 (1994) 17953.
- 339 [20] G. Kresse, D. Joubert, *Physical Review B* 59 (1999) 1758.
- 340 [21] G. Kresse, J. Furthmüller, *Physical Review B* 54 (1996) 11169.
- 341 [22] M.H.F. Sluiter en Y. Kawazoe, *Europhys. Lett.* 57 (2002) 526–532.
- 342 343
- 344 [23] A. Zunger, S. Wei, L. Ferreira, J. Bernard, *Physical Review Letters* 65 (1990) 353–356.
- 345 [24] S. Müller, *Journal of Physics: Condensed Matter* 15 (2003) R1429.
- 346 347
- 348 [25] P. E. A. Turchi, M. Sluiter, F. J. Pinski, D. D. Johnson, D. M. Nicholson, G. M. Stocks, J. B. Staunton, *Physical Review Letters* 67 (1991) 1779–1782.
- 349 350
- 351 [26] H. Okamoto, *Binary Alloys Phase Diagrams*, 2nd ed., 1990, pp. 772–773.
- 352 [27] National Institute for Materials Science (NIMS), *AtomWork*, 2012. [Http://crystdb.nims.go.jp/](http://crystdb.nims.go.jp/).
- 353 354
- 355 [28] Y. Xu, M. Yamazaki, P. Villars, *Japanese Journal of Applied Physics* 50 (2011) 11RH02.
- 356 [29] W. Witteman, A. Giorgi, D. Vier, *Journal of Physical Chemistry* 64 (1960) 434.
- 357 358
- 359 [30] A. Zastawny, J. Bialon, T. Sosinski, *Applied Radiation and Isotopes* 40 (1989) 19.
- 360 [31] T. Miura, T. Obara, H. Sekimoto, *Applied Radiation and Isotopes* 61 (2004) 1307.
- 361 362
- 363 [32] J. Neuhausen, D. Schumann, R. Dressler, B. Eichler, S. Heinitz, B. Hammer, F. von Rohr, L. Zanini, V. Boutellier, M. Rthi, J. Eikenberg, E. Noah, *Proceedings of the DAE-BRNS Symposium on Nuclear and Radiochemistry NUCAR-2011, Visakhapatnam* (2011) 44.
- 364 365 366
- 367 [33] G. Tammann, A. von Löwis of Menar, *Zeitschrift für anorganische und allgemeine Chemie* 205 (1932) 145.
- 368 369
- 370 [34] V. Kutznetsov, V. Zlomanov, *Inorganic Materials* 25 (1989) 923.
- 371 [35] K. Yamana, K. Kihara, T. Matsumoto, *Acta Crystallographica B* 35 (1979) 147.
- 372 [36] S. Chizhevskaya, L. Shelimova, V. Zemskov, V. Kosyakov, D. Malakhov, *Inorganic Materials* 30 (1994) 1.
- 373 374 375 376 377 378 379 380 381 382 383 384 385 386
- [37] R. Blachnik, F. Romermann, A. Schlieper, *Zeitschrift für Metallkunde* 88 (1997) 301.
- [38] R. Oshea, J. Donovan, E. Peretti, *Transactions of the Metallurgical Society of AIME* 221 (1961) 1266.
- [39] R. Oshea, E. Peretti, *Transactions of the American Society of Metals Quarterly* 56 (1963) 153.
- [40] W. Gierlotka, J. Lapsa, D. Jendrzeczyk-Handzlik, *Journal of Alloys and Compounds* 479 (2009) 152.
- [41] J. Goode, *Mound Laboratory Report 1952/55; N.S.A.* 10 (1956).
- [42] T. Miura, T. Obara, H. Sekimoto, *Annals of Nuclear Energy* 34 (2007) 926.
- [43] J. Neuhausen, U. Köster, B. Eichler, *Radiochimica Acta* 92 (2004) 917.